References and Notes

1. K. J. Hasenkrug, B. Chesebro, *Proc. Natl. Acad. Sci. U.S.A.* **94**, 7811 (1997).
2. W. Li, W. R. Green, *J. Virol.* **80**, 5777 (2006).
3. S. Best, P. Le Tissier, G. Towers, J. P. Stoye, *Nature* **382**, 826 (1996).
4. D. A. Persons *et al.*, *Nat. Genet.* **23**, 159 (1999).
5. W. J. Britt, B. Chesebro, *J. Exp. Med.* **157**, 1736 (1983).
6. B. Chesebro, K. Wehrly, in *Advances in Comparative Leukemia Research*, P. Bentvelzen, Ed. (North-Holland Biomedical Press, Elsevier, 1978), pp. 69–73.
7. B. Chesebro, K. Wehrly, *Proc. Natl. Acad. Sci. U.S.A.* **76**, 425 (1979).
8. D. Doig, B. Chesebro, *J. Exp. Med.* **150**, 10 (1979).
9. K. J. Hasenkrug, *J. Virol.* **73**, 6468 (1999).
10. K. J. Hasenkrug *et al.*, *J. Virol.* **69**, 2617 (1995).
11. H. J. Super *et al.*, *J. Virol.* **73**, 7848 (1999).
12. Y. Kanari *et al.*, *AIDS* **19**, 1015 (2005).
13. Y. L. Chiu, W. C. Greene, *Annu. Rev. Immunol.* **26**, 317 (2008).
14. Materials and methods are available as supporting material on *Science* Online.
15. B. Chesebro, K. Wehrly, *J. Exp. Med.* **143**, 73 (1976).
16. H. C. Van der Gaag, A. A. Axelrad, *Virology* **177**, 837 (1990).
17. S. J. Rulli Jr. *et al.*, *J. Virol.* **82**, 6566 (2008).
18. J. L. Portis, F. J. McAtee, S. C. Kayman, *J. Acquir. Immune Defic. Syndr.* **5**, 1272 (1992).
19. J. G. Monroe, A. Lowy, R. D. Granstein, M. I. Greene, *Immunol. Rev.* **80**, 103 (1984).
20. A. Gonzalez-Fernandez, C. Milstein, *Immunology* **93**, 149 (1998).
21. Y. T. Kim, G. W. Siskind, *Clin. Exp. Immunol.* **17**, 329 (1974).
22. M. Muramatsu *et al.*, *Cell* **102**, 553 (2000).
23. K. Stopak, C. de Noronha, W. Yonemoto, W. C. Greene, *Mol. Cell* **12**, 591 (2003).
24. M. Marin, K. M. Rose, S. L. Kozak, D. Kabat, *Nat. Med.* **9**, 1398 (2003).
25. A. M. Sheehy, N. C. Gaddis, M. H. Malim, *Nat. Med.* **9**, 1404 (2003).
26. Y. H. Zheng *et al.*, *J. Virol.* **78**, 6073 (2004).
27. D. R. Burton *et al.*, *Nat. Immunol.* **5**, 233 (2004).

28. We thank the Transgenic Core Laboratory, the Animal Facility, and S. Espineda at the J. David Gladstone Institutes for technical assistance; L. Evans, J. Portis, R. Gallo, R. Locksley, and members of the Greene and Hasenkrug Laboratory for helpful discussions; and R. Givens, S. Cammack, and G. Howard for manuscript preparation. This work was supported by the NIAID Division of Intramural Research at NIH to K.J.H. and B.C., an NIH R01 AI065329 to W.C.G., and an NIH facility grant to the J. David Gladstone Institutes. Sequences are deposited in GenBank, with accession numbers EU707568 to EU707571.

Supporting Online Material

www.sciencemag.org/cgi/content/full/321/5894/1343/DC1
Materials and Methods
SOM Text
Figs. S1 to S6
Table S1
References

29 May 2008; accepted 24 July 2008
10.1126/science.1161121

Human-Specific Gain of Function in a Developmental Enhancer

Shyam Prabhakar,[1]* Axel Visel,[1] Jennifer A. Akiyama,[1] Malak Shoukry,[1] Keith D. Lewis,[1]† Amy Holt,[1] Ingrid Plajzer-Frick,[1] Harris Morrison,[2] David R. FitzPatrick,[2] Veena Afzal,[1] Len A. Pennacchio,[1,3] Edward M. Rubin,[1,3]‡ James P. Noonan[1]‡§

Changes in gene regulation are thought to have contributed to the evolution of human development. However, in vivo evidence for uniquely human developmental regulatory function has remained elusive. In transgenic mice, a conserved noncoding sequence (*HACNS1*) that evolved extremely rapidly in humans acted as an enhancer of gene expression that has gained a strong limb expression domain relative to the orthologous elements from chimpanzee and rhesus macaque. This gain of function was consistent across two developmental stages in the mouse and included the presumptive anterior wrist and proximal thumb. In vivo analyses with synthetic enhancers, in which human-specific substitutions were introduced into the chimpanzee enhancer sequence or reverted in the human enhancer to the ancestral state, indicated that 13 substitutions clustered in an 81–base pair module otherwise highly constrained among terrestrial vertebrates were sufficient to confer the human-specific limb expression domain.

Genome sequence changes that altered the molecular machinery of development likely facilitated the evolution of uniquely human morphological traits (*1*, *2*). Although these genetic modifications remain largely unidentified, it has long been thought that they included changes in gene expression due to positive selection for nucleotide substitutions that altered the activity of cis-regulatory elements (*3*). Several cases of putatively adaptive sequence change, including polymorphisms among human populations and apparently fixed differences between humans and other primates, have been shown to affect in vitro promoter or enhancer function in cell line reporter assays (*4*–*7*). However, the impact of human-specific nucleotide substitutions on the in vivo activity of developmental regulatory elements remains obscure.

In vivo analyses of evolutionarily conserved noncoding sequences have revealed them to be enriched in cis-regulatory transcriptional enhancers that confer specific expression patterns during development (*8*–*11*). Recent efforts have identified conserved noncoding sequences that evolved rapidly on the human lineage, but it is not known whether these sequences include regulatory elements with altered activities in humans (*12*–*15*). Here, we focus on functionally characterizing the most rapidly evolving human noncoding element yet identified, which we termed human-accelerated conserved noncoding sequence 1 (*HACNS1*) (*12*). Although this 546–base pair (bp) element is highly constrained in all sequenced terrestrial vertebrate genomes, it has accumulated 16 human-specific sequence changes in the ~6 million years since the human-chimpanzee split (Fig. 1A). We evaluated the significance of this evolutionary acceleration by means of a test statistic that represents the log-likelihood, or information theoretic "surprisal," of observing the human sequence given the orthologous sequences from multiple terrestrial vertebrates. Assuming *HACNS1* is under functional constraint in humans, its rapid divergence is highly unexpected given its strong conservation in these other species [surprisal test P value = 9.2×10^{-12} (*16*)]. This divergence also significantly exceeds the ~4 substitutions expected if *HACNS1* were evolving at the neutral substitution rate in humans [surprisal test P value = 1.3×10^{-6} (*16*)]. One explanation for this marked acceleration is that *HACNS1* has undergone several instances of positive selection during human evolution that may have altered its function.

To test this hypothesis, we evaluated the ability of *HACNS1* and its orthologs from chimpanzee and rhesus macaque to function as transcriptional enhancers during development, using a transgenic mouse enhancer assay in which the activity of each sequence is assessed through a β-galactosidase (*lacZ*) reporter gene coupled to a minimal *Hsp68* promoter (*17*). We initially examined the potential enhancer activity of *HACNS1* at embryonic day 11.5 (E11.5). We tested a 1.2-kb DNA fragment encompassing *HACNS1* that also contained nonconserved sequences flanking the element, in order to include possible functional sequences near *HACNS1* not detected by conservation (table S1). At E11.5, the human element drove strong and reproducible reporter gene expression in the anterior limb bud, pharyngeal arches, and developing ear and eye, which suggests that *HACNS1* acts as a robust enhancer during development (Fig. 1, B and C, and fig. S1). In striking contrast to the highly reproducible staining driven by the human enhancer, which extended into the most distal region of the anterior limb bud in five of six lacZ-positive embryos (Fig. 1C and *HACNS1* embryos

[1]Genomics Division, Lawrence Berkeley National Laboratory, Berkeley, CA 94720, USA. [2]MRC Human Genetics Unit, Western General Hospital, Edinburgh EH4 2XU, UK. [3]United States Department of Energy Joint Genome Institute, Walnut Creek, CA 94598, USA.

*Present address: Computational and Mathematical Biology, Genome Institute of Singapore 138672, Singapore.
†Present address: Division of Biology, California Institute of Technology, Pasadena, CA 91125, USA.
‡To whom correspondence should be addressed. E-mail: emrubin@lbl.gov (E.M.R.); james.noonan@yale.edu (J.P.N.)
§Present address: Department of Genetics, Yale University School of Medicine, New Haven, CT 06520, USA.

1 to 5 in fig. S1), the chimpanzee and rhesus orthologs failed to drive reproducible reporter gene expression in the distal limb bud, although they did drive moderately reproducible expression at the base of the limb (Fig. 1, B and C; chimpanzee enhancer embryos 1, 2, 6, 7, and 8 and rhesus enhancer embryos 1 to 4, 6 to 8, and 10 in fig. S1).

Two of the embryos that were transgenic for the chimpanzee ortholog and showed this pattern also exhibited diffuse, low-level staining that extended into the anterior limb, which suggests that the chimpanzee enhancer may possess a weak capacity to drive expression in this structure (embryos 6 and 7 in fig. S1). However, this infrequent pattern was in stark contrast to the strong and highly reproducible pattern of the human enhancer. Furthermore, pharyngeal arch, eye, and ear expression was less reproducible and, where present, generally weaker in multiple positive embryos for both nonhuman orthologs; these findings suggest additional sites of reduced overall enhancer activity relative to the human ortholog.

To assess the *HACNS1* limb expression pattern at higher resolution, we sectioned *HACNS1* transgenic embryos and found that staining in the forelimb was restricted to the mesenchyme, forming a continuous expression domain that extended deep into the limb bud along the anteroposterior axis at the handplate and shoulder while remaining more anterior in between (fig. S3). These results provide evidence that the human-specific sequence changes in *HACNS1* have resulted in a gain of function in this otherwise highly conserved enhancer, increasing its overall robustness and producing a strong human-specific expression domain in the anterior limb bud mesenchyme at E11.5. Because the chimpanzee and rhesus orthologs yield similar patterns to each other and show consistent differences relative to *HACNS1*, a parsimonious conclusion would be that the chimpanzee and rhesus patterns reflect the ancestral primate state from which the human-specific pattern has evolved.

To explore the activity of *HACNS1* at a more advanced stage of limb development, we compared the expression patterns of the human, chimpanzee, and rhesus enhancers in E13.5 transgenic mouse embryos. At this stage, the human element continued to drive reproducible reporter gene expression in the anterior developing forelimb, particularly in the shoulder and the anterior junction of the forearm and handplate, in 11 of 12 positive embryos (Fig. 2, A to C; embryos 1 to 10 and 12 in fig. S2). In four of these embryos, the reporter gene activity extended into the future anterior-most digit of the forelimb (Fig. 2B). Similar expression, although with weaker staining, was also observed in the corresponding structures in the hindlimb. Imaging of lacZ staining in a representative *HACNS1* transgenic embryo by means of optical projection tomography [OPT (*18*)] revealed that the anterior expression evident in the whole mount extended deep inside the limb at the forearm-handplate junction (fig. S4). The orthologous chimpanzee and rhesus elements failed to drive reproducible expression in the distal limbs at this time point, although a subset of positive embryos in each case (4 of 10 for chimpanzee; 3 of 12 for rhesus) showed reporter gene expression in the shoulder region of the limb bud, thus recapitulating the proximal tip of the expression domain of the human enhancer (Fig. 2A; chimpanzee enhancer embryos 2 to 5 and rhesus enhancer embryos 1, 5, and 6 in fig. S2). OPT imaging confirmed the absence of reproducible lacZ staining inside the distal limb in representative embryos transgenic for the rhesus and chimpanzee enhancers (fig. S4). These results indicate that the human-specific enhancer activity persists across multiple developmental stages. Moreover, they suggest that the robust anterior limb expression pattern of *HACNS1* evolved from a weaker ancestral pattern that is largely confined to the base of the limb bud, as evident in the

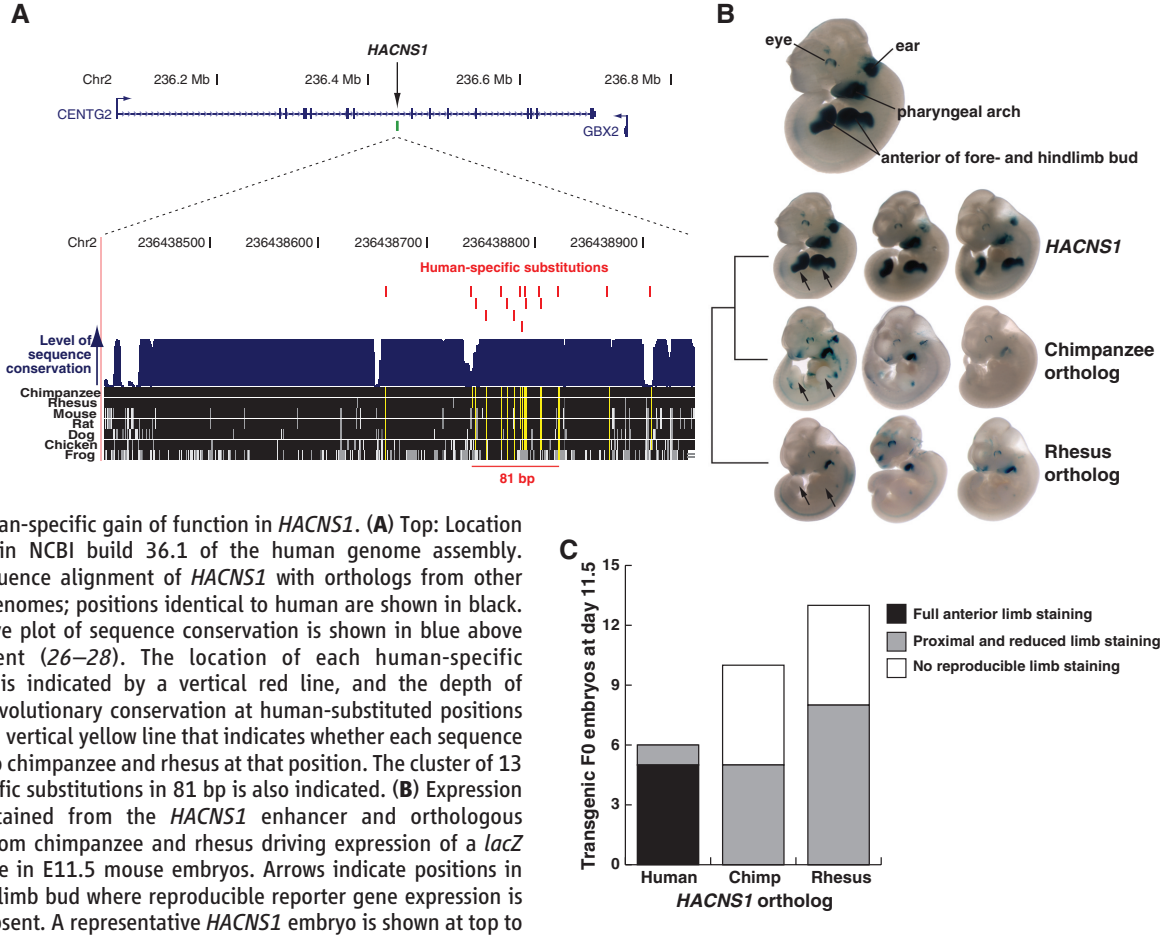

Fig. 1. Human-specific gain of function in *HACNS1*. (**A**) Top: Location of *HACNS1* in NCBI build 36.1 of the human genome assembly. Bottom: Sequence alignment of *HACNS1* with orthologs from other vertebrate genomes; positions identical to human are shown in black. A quantitative plot of sequence conservation is shown in blue above the alignment (*26*–*28*). The location of each human-specific substitution is indicated by a vertical red line, and the depth of nonhuman evolutionary conservation at human-substituted positions is shown by a vertical yellow line that indicates whether each sequence is identical to chimpanzee and rhesus at that position. The cluster of 13 human-specific substitutions in 81 bp is also indicated. (**B**) Expression patterns obtained from the *HACNS1* enhancer and orthologous sequences from chimpanzee and rhesus driving expression of a *lacZ* reporter gene in E11.5 mouse embryos. Arrows indicate positions in the anterior limb bud where reproducible reporter gene expression is present or absent. A representative *HACNS1* embryo is shown at top to illustrate the relevant anatomical structures. Three embryos resulting from independent transgene integration events are shown for each orthologous sequence tested. (**C**) Number of embryos transgenic for each sequence displaying the limb expression patterns described in the text.

activities of the chimpanzee and rhesus enhancers at both time points.

We next sought to identify human-specific sequence changes responsible for the functional change in the human enhancer. Although the 16 human-specific substitutions within the 546-bp conserved region corresponding to *HACNS1* are the most striking feature of the 1.2-kb orthologous segments we initially tested for enhancer function, these segments also included ~650 bp of nonconserved DNA containing additional human-chimpanzee sequence differences. To isolate the effect of the substitutions within *HACNS1* on enhancer function, we synthesized a chimeric 1.2-kb enhancer in which we transferred all 16 substitutions into the chimpanzee sequence background (*16*). This "humanized" chimpanzee enhancer produced an E11.5 expression pattern nearly identical to that of the native human enhancer; this finding suggests that the human-specific sequence changes within *HACNS1* are responsible for the gain of function we observed (8 of 8 embryos; Fig. 3D and fig. S1). Strikingly, these human-specific substitutions were significantly clustered: 13 of 16 substitutions occurred within an 81-bp region of the 546-bp conserved element [permutation test P value = 1.7×10^{-7} (*16*)], which suggests that this region may be particularly relevant to the human-specific function of *HACNS1* (Figs. 1A and 3A).

To test this hypothesis, we synthesized a chimeric 1.2-kb enhancer in which the 13 clustered human substitutions were introduced into the chimpanzee sequence background (table S2). At E11.5, this element produced an anterior limb bud pattern highly similar to the *HACNS1* pattern (6 of 6 positive embryos; Fig. 3 and fig. S1). We also performed the reciprocal experiment, synthesizing a complementary chimeric enhancer where we replaced the 13 human-specific nucleotides in the human enhancer sequence with their putatively ancestral orthologs from chimpanzee. This "reverted" enhancer yielded a pattern very similar to the chimpanzee and rhesus enhancer patterns shown in Fig. 1B, with expression in the anterior limb bud greatly reduced or absent (Fig. 3 and fig. S1). These results confirm the robustness of the functional differences we observed between *HACNS1* and its chimpanzee and rhesus orthologs, and they indicate that the *HACNS1* anterior limb bud pattern is largely attributable to one or more of the 13 clustered human-specific substitutions we identified. To further dissect the functional contribution of these substitutions, we introduced independent groups of six substitutions and three substitutions into the chimpanzee enhancer sequence (fig. S5). These enhancers drove variable expression in the anterior limb bud, which suggests that at least two human-specific substitutions are required for the gain of function in *HACNS1*.

The precise molecular mechanism by which the substitutions in *HACNS1* confer the human-specific expression pattern remains to be determined. Computational analysis of predicted transcription factor binding sites in *HACNS1* and its nonhuman orthologs suggested that multiple sites have been gained and lost in this enhancer during human evolution (fig. S6). Predicted human-specific binding sites for the developmental transcription factors PAX9 and ZNF423 may contribute to *HACNS1* enhancer activity, given that the known expression pattern of *PAX9* in the mouse limb overlaps the human-specific limb domain of *HACNS1* at E11.5 and E13.5, and *ZNF423* is expressed in the mouse handplate mesenchyme from E10.5 through E12.5 (*19*–*21*).

Multiple lines of evidence suggest that the functional changes in *HACNS1* are due to adaptive evolution. The rate of human-specific accelerated evolution in *HACNS1* is more than 4 times the local neutral rate. Moreover, this rapid evolution cannot be explained purely on the basis of biased gene conversion (BGC), a neutral mechanism postulated to cause hotspots of accelerated evolution in the genome by increasing the local fixation rate of AT → GC substitutions (*22*, *23*). Under the neutral BGC hypothesis, one would expect an increase in the overall substitution rate across the entire region of increased AT → GC substitution (*23*). An excess of AT → GC substitutions is indeed present in *HACNS1* [binomial test P value = 1.1×10^{-4} (*16*)], and the element lies in a ~5-kb genomic region enriched in such substitutions (Fig. 4). However, the human-specific substitution rate is elevated only in the narrow 81-bp region in *HACNS1* described above and is close to the local average outside of this window (Fig. 4). These data, coupled with the human-specific functional changes in *HACNS1*, argue against a purely neutral explanation for the rapid evolution of this element in humans.

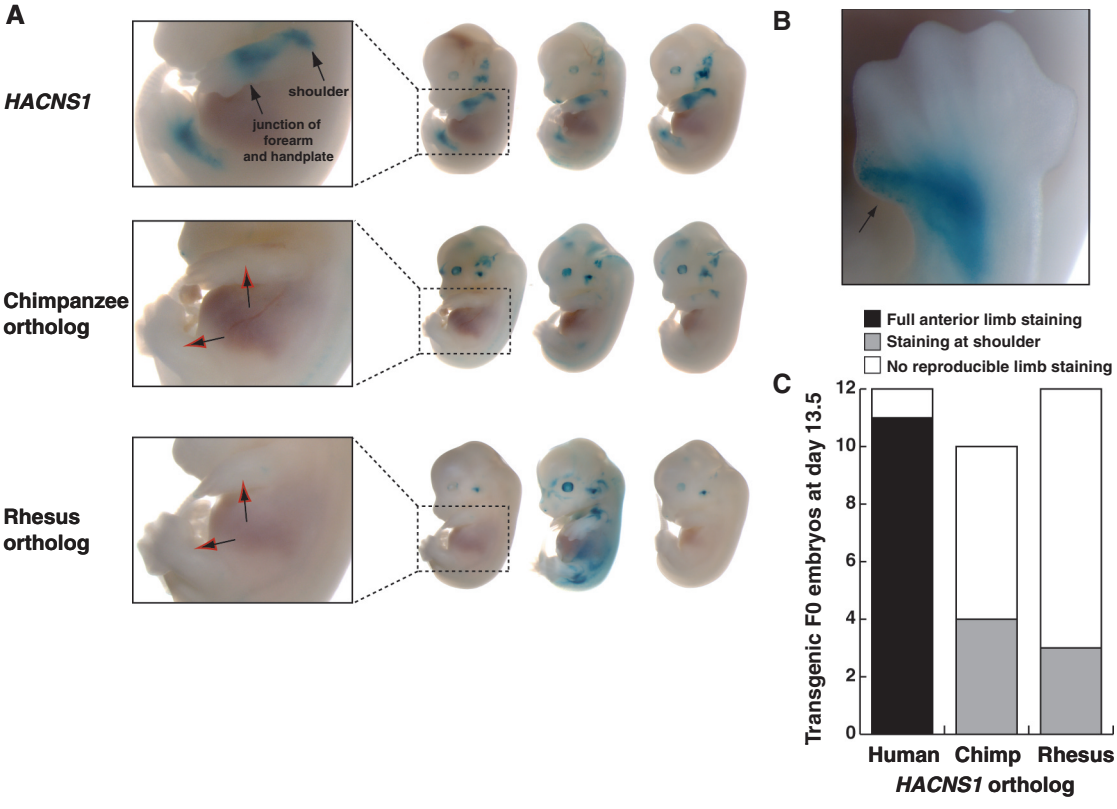

Fig. 2. Gain of function in *HACNS1* persists at E13.5. (**A**) Expression patterns obtained from *HACNS1* and its chimpanzee ortholog in E13.5 mouse embryos. Three embryos resulting from independent transgene integration events are shown for each construct. Close-up views of forelimb and hindlimb expression in a representative embryo for each construct are shown at left, and arrows indicate positions where limb expression is present or absent. (**B**) Dorsal view of reporter gene expression in the distal anterior forelimb of a *HACNS1* E13.5 transgenic embryo. Arrow indicates the most anterior digit. (**C**) Number of embryos transgenic for each construct that display the limb expression patterns described in the text.

Our results evoke the hypothesis that human-specific adaptive evolution in *HACNS1* has contributed to uniquely human aspects of digit and limb patterning. The dexterity of the human hand is due to morphological differences compared with other primates that include rotation of the thumb toward the palm and an increase in the length of the thumb relative to the other digits (*1*). Human-specific changes in hindlimb morphology, such as the characteristic inflexibility and shortened digits of the human foot, facilitated habitual bipedalism. The gain of function in *HACNS1* may have influenced the evolution of these or other human limb features by altering the expression of nearby genes during limb development. *HACNS1* is located within an intron of *CENTG2*, which encodes a guanosine triphosphatase activating protein involved in the regulation of endosome function. The next-closest gene is *GBX2*, which is located ~300 kb downstream of *HACNS1* and encodes an essential developmental transcription factor (*24*, *25*). The role of *CENTG2* in limb development has not been evaluated. Mouse *Gbx2* is expressed in the developing limb, but *Gbx2* null mice have not been described as showing abnormal limbs (*25*). The potential impact of human-specific changes in the expression of these genes on limb development thus remains to be explored. We also note that the *HACNS1* expression pattern in transgenic mice may not entirely recapitulate the precise *HACNS1* expression pattern in the human embryo. We therefore cannot rule out the possibility that the accelerated evolution of *HACNS1* reflects selection for changes in structures other than, or in addition to, the limb. Elucidating the role of *HACNS1* in human morphological evolution requires further lines of evidence, including the analysis of *GBX2* and *CENTG2* expression during human development and the generation of *HACNS1* targeted replacement mice. Independent of these considerations, our study suggests that adaptive nucleotide substitution altered the function of a developmental enhancer in humans, and illustrates a strategy that could be used across the genome to understand at a molecular level how human development evolved through cis-regulatory change.

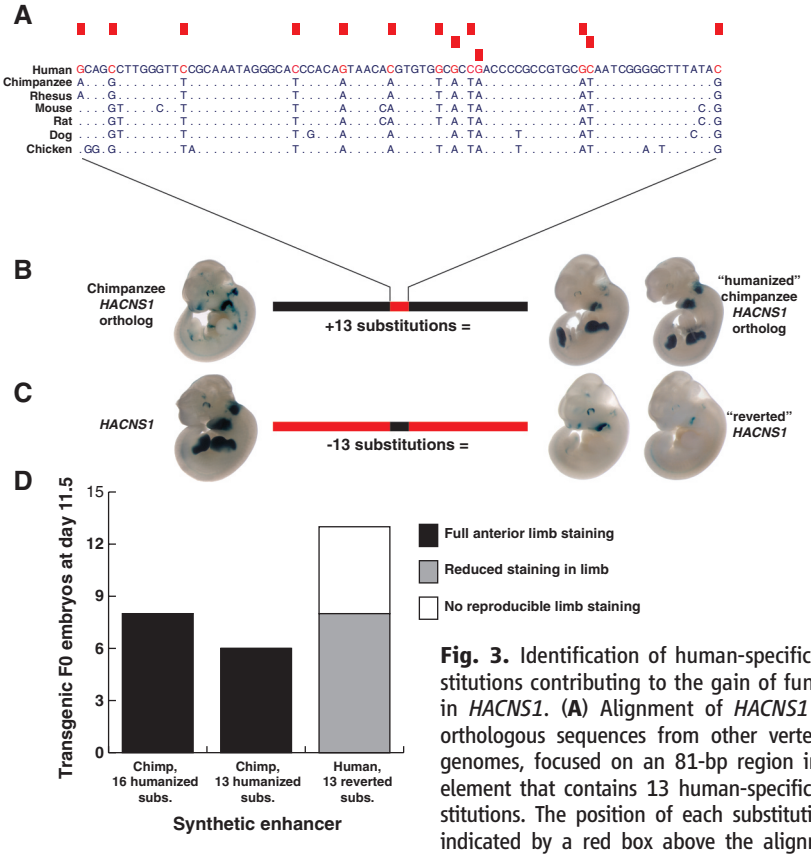

Fig. 3. Identification of human-specific substitutions contributing to the gain of function in *HACNS1*. (**A**) Alignment of *HACNS1* with orthologous sequences from other vertebrate genomes, focused on an 81-bp region in the element that contains 13 human-specific substitutions. The position of each substitution is indicated by a red box above the alignment; each human-specific nucleotide is highlighted in red. Positions in the nonhuman genomes that are identical to the human sequence are displayed as dots. (**B**) Expression pattern of a synthetic enhancer in which the 13 human-specific substitutions (red box) are introduced into the orthologous 1.2-kb chimpanzee sequence background (black bar). (**C**) Expression pattern of a synthetic enhancer obtained by reversion of these substitutions (black box) in the human sequence (red bar) to the nucleotide states in chimpanzee and rhesus. (**D**) Number of embryos transgenic for each synthetic enhancer that show full, partial, or no expression in the limb at E11.5.

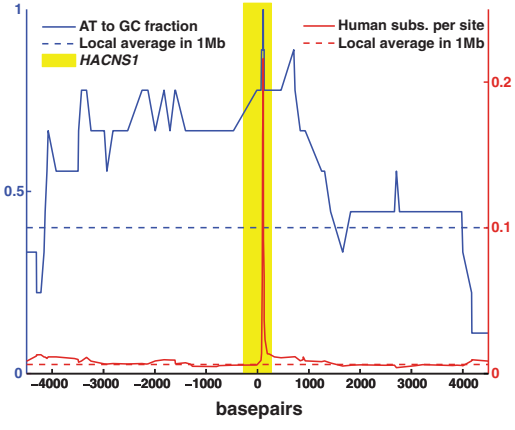

Fig. 4. Human-specific substitution rate and proportion of AT → GC substitutions in *HACNS1* and flanking genomic region. The rate of human-specific substitutions (solid red line) and the fraction of human substitutions that are AT → GC events (solid blue line) were estimated in sliding windows across a 9-kb interval around *HACNS1*. The average values of each metric for 1 Mb of genomic sequence centered on *HACNS1* are shown for reference (dashed lines). The 546-bp interval corresponding to *HACNS1* is highlighted in yellow.

References and Notes

1. E. Trinkaus, in *The Cambridge Encyclopedia of Human Evolution*, S. Jones, R. Martin, D. Pilbeam, Eds. (Cambridge Univ. Press, New York, 1993), pp. 346–349.
2. S. B. Carroll, *Nature* **422**, 849 (2003).
3. M. C. King, A. C. Wilson, *Science* **188**, 107 (1975).
4. C. Tournamille *et al.*, *Nat. Genet.* **10**, 224 (1995).
5. M. V. Rockman *et al.*, *PLoS Biol.* **3**, e387 (2005).
6. S. A. Tishkoff *et al.*, *Nat. Genet.* **39**, 31 (2007).
7. G. A. Wray, *Nat. Rev. Genet.* **8**, 206 (2007).
8. D. Boffelli, M. A. Nobrega, E. M. Rubin, *Nat. Rev. Genet.* **5**, 456 (2004).
9. M. A. Nobrega, I. Ovcharenko, V. Afzal, E. M. Rubin, *Science* **302**, 413 (2003).
10. L. A. Pennacchio *et al.*, *Nature* **444**, 499 (2006).
11. A. Visel *et al.*, *Nat. Genet.* **40**, 158 (2008).
12. S. Prabhakar, J. P. Noonan, S. Pääbo, E. M. Rubin, *Science* **314**, 786 (2006).
13. K. S. Pollard *et al.*, *Nature* **443**, 167 (2006).
14. C. P. Bird *et al.*, *Genome Biol.* **8**, R118 (2007).
15. E. C. Bush, B. T. Lahn, *BMC Evol. Biol.* **8**, 17 (2008).
16. See supporting material on *Science* Online.
17. R. Kothary *et al.*, *Development* **105**, 707 (1989).
18. J. Sharpe *et al.*, *Science* **296**, 541 (2002).
19. A. Neubüser, H. Koseki, R. Balling, *Dev. Biol.* **170**, 701 (1995).
20. H. Peters, A. Neubüser, K. Kratochwil, R. Balling, *Genes Dev.* **12**, 2735 (1998).
21. S. Warming, T. Suzuki, T. P. Yamaguchi, N. A. Jenkins, N. G. Copeland, *Oncogene* **23**, 2727 (2004).
22. K. S. Pollard *et al.*, *PLoS Genet.* **2**, e168 (2006).
23. N. Galtier, L. Duret, *Trends Genet.* **23**, 273 (2007).
24. Z. Nie *et al.*, *J. Biol. Chem.* **277**, 48965 (2002).
25. K. M. Wassarman *et al.*, *Development* **124**, 2923 (1997).
26. M. Blanchette *et al.*, *Genome Res.* **14**, 708 (2004).
27. A. Siepel *et al.*, *Genome Res.* **15**, 1034 (2005).
28. W. J. Kent *et al.*, *Genome Res.* **12**, 996 (2002).

29. We thank members of the Pennacchio and Rubin laboratories for critical comments on the manuscript. Research was done under Department of Energy Contract

DE-AC02-05CH11231, University of California, E. O. Lawrence Berkeley National Laboratory, and supported by National Heart, Lung and Blood Institute grant HL066681 and National Human Genome Research Institute grant HG003988 (L.A.P.); the Agency for Science, Technology, and Research of Singapore (S.P.); an American Heart Association postdoctoral fellowship (A.V.); and NIH National Research Service Award fellowship 1-F32-GM074367 and the Department of Genetics, Yale University School of Medicine (J.P.N.).

Supporting Online Material
www.sciencemag.org/cgi/content/full/321/5894/1346/DC1
Materials and Methods
Figs. S1 to S6
Table S1
References

2 May 2008; accepted 7 July 2008
10.1126/science.1159974

Wnt3a-Mediated Formation of Phosphatidylinositol 4,5-Bisphosphate Regulates LRP6 Phosphorylation

Weijun Pan,[1]* Sun-Cheol Choi,[2]* He Wang,[3]* Yuanbo Qin,[3] Laura Volpicelli-Daley,[4] Laura Swan,[4] Louise Lucast,[4] Cynthia Khoo,[5] Xiaowu Zhang,[6] Lin Li,[3] Charles S. Abrams,[5] Sergei Y. Sokol,[2] Dianqing Wu[1]†

The canonical Wnt–β-catenin signaling pathway is initiated by inducing phosphorylation of one of the Wnt receptors, low-density lipoprotein receptor-related protein 6 (LRP6), at threonine residue 1479 (Thr^{1479}) and serine residue 1490 (Ser^{1490}). By screening a human kinase small interfering RNA library, we identified phosphatidylinositol 4-kinase type II α and phosphatidylinositol-4-phosphate 5-kinase type I (PIP5KI) as required for Wnt3a-induced LRP6 phosphorylation at Ser^{1490} in mammalian cells and confirmed that these kinases are important for Wnt signaling in *Xenopus* embryos. Wnt3a stimulates the formation of phosphatidylinositol 4,5-bisphosphates [PtdIns (4,5)P_2] through frizzled and dishevelled, the latter of which directly interacted with and activated PIP5KI. In turn, PtdIns (4,5)P_2 regulated phosphorylation of LRP6 at Thr^{1479} and Ser^{1490}. Therefore, our study reveals a signaling mechanism for Wnt to regulate LRP6 phosphorylation.

Members of the Wnt family of secretory glycoproteins have important roles in various physiological and pathophysiological processes, including embryonic development, bone development, neuronogenesis, adipogenesis, myogenesis, organogenesis, lipid and glucose metabolism, and tumorigenesis (*1*–*5*). Canonical Wnt binds to two receptors, lipoprotein receptor-related protein 6 (LRP6) and frizzled (Fz) proteins, leading to phosphorylation of LRP6 at Thr^{1479} by casein kinase 1γ and at Ser^{1490} by glycogen synthase kinase 3 (GSK3) (*6*–*10*). Wnt appears to regulate Thr^{1479} phosphorylation by inducing the formation of LRP6 aggregates (*9*), whereas it regulates Ser^{1490} phosphorylation through GSK in an axin-dependent manner (*10*). To determine whether there are other kinases that take part in the regulation of LRP6 phosphorylation, we screened a human kinase small in-

[1]Department of Pharmacology, Yale University School of Medicine, New Haven, CT 06510, USA. [2]Department of Developmental and Regenerative Biology, Mount Sinai School of Medicine, New York, NY 10029, USA. [3]State Key Laboratory of Molecular Biology and Center of Cell Signaling, Institute of Biochemistry and Cell Biology, Shanghai Institutes for Biological Sciences, Chinese Academy of Sciences, Shanghai 200031, China. [4]Department of Cell Biology and Howard Hughes Medical Institute, Yale University School of Medicine, New Haven, CT 06510, USA. [5]Department of Medicine, University of Pennsylvania, Philadelphia, PA 19104, USA. [6]Cell Signaling Technology, Danvers, MA 01923, USA.

*These authors contribute equally to this work.
†To whom correspondence should be addressed. E-mail: dan.wu@yale.edu

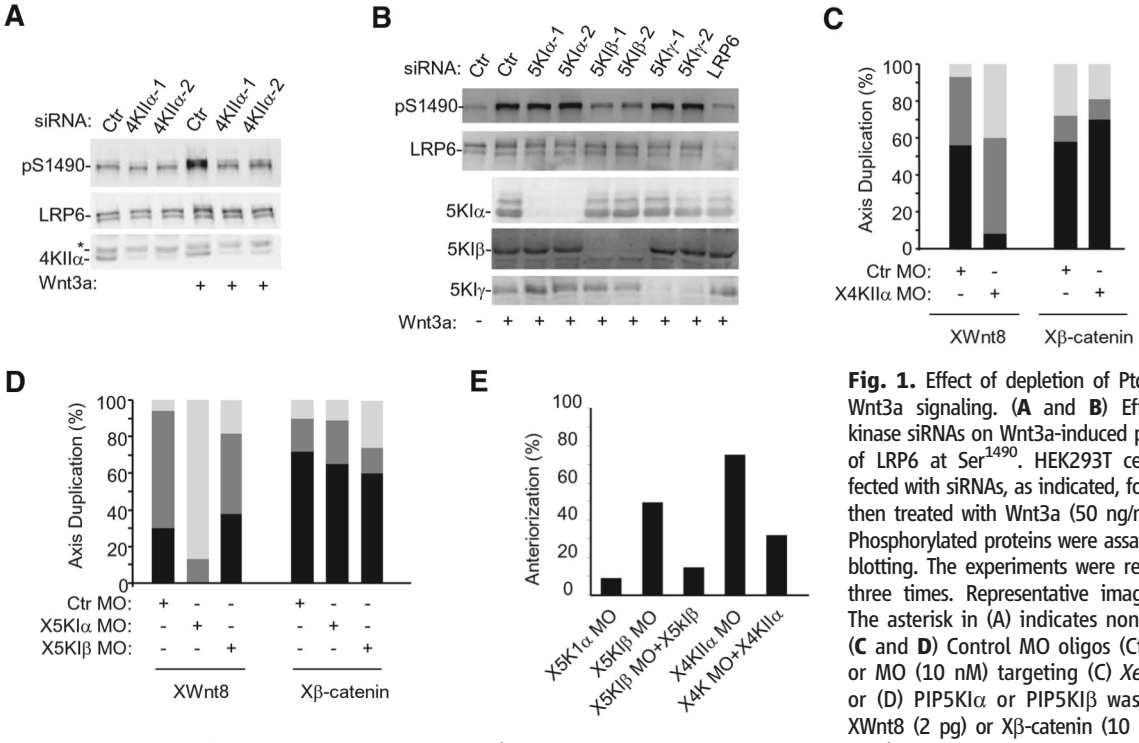

Fig. 1. Effect of depletion of PtdIns kinases on Wnt3a signaling. (**A** and **B**) Effects of PtdIns kinase siRNAs on Wnt3a-induced phosphorylation of LRP6 at Ser^{1490}. HEK293T cells were transfected with siRNAs, as indicated, for 48 hours and then treated with Wnt3a (50 ng/ml) for 30 min. Phosphorylated proteins were assayed by Western blotting. The experiments were repeated at least three times. Representative images are shown. The asterisk in (A) indicates nonspecific bands. (**C** and **D**) Control MO oligos (Ctr MO, 10 nM) or MO (10 nM) targeting (C) *Xenopus* PI4KIIα or (D) PIP5KIα or PIP5KIβ was injected with XWnt8 (2 pg) or Xβ-catenin (10 pg) mRNA into four-cell stage embryos. $n > 40$ for all of the *Xenopus* embryo studies (where n is the number of examined embryos). Open bars, no double axis; light gray bars, incomplete double axis; black bars, complete double axis. (**E**) Four-cell stage embryos were injected with XPIP5KIβ MO (40 ng), XPI4KIIα MO (40 ng), or XPIP5KIα MO (40 ng) with or without XPIP5KIβ (10 pg) or XPI4KIIα (5 pg) RNA in the dorsal region and cultured to tailbud stages. XPIP5KIα MO, $n = 30$; XPIP5KIβ MO, $n = 45$; XPIP5KIβ MO+XPIP5KIβ, $n = 29$; XPI4KIIα MO, $n = 55$; and XPI4KIIα MO+XPI4KIIα, $n = 30$.